Journal of Holography Applications in Physics
Volume 7, Issue 2, Spring 2027, xx–xx
©Available online at http://jhap.du.ac.ir
DOI: 10.22128/jhap.2026.3362.1209
Online ISSN: 2783–3518

Regular article

Reconstruction of Cosmological Models from Hubble Parameter in $f(Q,T)$ Gravity

Adesh Meshram[1] · Praveen Kumar Dhankar[2] · Rekha Patel[3] · Safiqul Islam[4] · Albert Munyeshyaka[5]

[1] Symbiosis Institute of Technology, Nagpur Campus, Symbiosis International (Deemed University), Pune-440008, Maharashtra, India;
Email: adeshmeshram1@gmail.com

[2] Symbiosis Institute of Technology, Nagpur Campus, Symbiosis International (Deemed University), Pune-440008, Maharashtra, India;
Corresponding Author E-mail: pkumar6743@gmail.com

[3] Symbiosis Institute of Technology, Nagpur Campus, Symbiosis International (Deemed University), Pune-440008, Maharashtra, India;
E-mail: patelrekha9256@gmail.com

[4] Department of Mathematics and Statistics, College of Science, King Faisal University, P.O. Box 400, Al Ahsa 31982, Saudi Arabia;
E-mail: sislam@kfu.edu.sa

[5] Rwanda Astrophysics, Space and Climate Science Research Group, University of Rwanda, College of Science and Technology, Kigali, Rwanda;
Department of educational sciences, Faculty of education, Mount Kigali University, Kigali, Rwanda;
E-mail: munalph@gmail.com

Received: June 16, 2026; **Revised:** August 12, 2026; **Accepted:** August 12, 2026

Abstract. In this work, we investigate the cosmological dynamics of the $f(Q,T) = \alpha Q+\beta T$ gravity model by considering a time-dependent scale factor as $a(t) = (\sinh(\lambda t))^{1/n}$. The corresponding field equations are solved to obtain the cosmological parameters in terms of redshift. The model parameters are constrained employing observational datasets consisting of Hubble, DESI BAO, and Union3 supernova data using the Markov Chain Monte Carlo (MCMC) method. The physical behavior of the derived model is examined by analysis of the deceleration parameter,pressure, energy density, equation of state parameter, and the $Om(z)$ diagnostic, while the physical credibility of the model is investigated using the energy conditions. Collectively, the model provides a consistent description of the accelerated expansion of the Universe at late-times and remains compatible based on observational data.

Keywords: Modified Gravity; $f(Q,T)$ Gravity; Data Analysis; MCMC.

COPYRIGHTS: ©2027, Journal of Holography Applications in Physics. Published by Damghan University. This article is an open-access article distributed under the terms and conditions of the Creative Commons Attribution 4.0 International (CC BY 4.0).
https://creativecommons.org/licenses/by/4.0

Article in press

Contents

1 Introduction **3**

2 Framework of $f(Q, T)$ Gravity and Solution of Field Equations **4**

3 Mathematical Formulation, cosmological evolution and Dynamical Quantities **6**

3.1 Model Discrimination via the $Om(z)$ Diagnostic 10
3.2 Analysis of Energy Conditions 11

4 Observational Viability of the Model **12**

5 Results and Discussion **18**

6 Conclusion **19**

References **20**

Article in press

1 Introduction

Understanding the dynamical evolution of the Universe remains one of the central problems in modern cosmology, particularly in explaining its transition from an early decelerated phase to the present accelerated phase [1,2]. This transition has been strongly supported by various independent observations, which have significantly shaped our current understanding of cosmic dynamics [3]. Observational evidence from Type Ia Supernovae [1,2,4], cosmic microwave background radiation [5,6], and baryon acoustic oscillations [7,8] has firmly established that the Universe is currently undergoing an accelerated expansion phase [9–11]. This unexpected behavior has motivated extensive efforts to identify a consistent theoretical framework capable of explaining the late-time acceleration of the Universe [3,12,13]. Although General Relativity has been highly successful in describing gravitational phenomena, it faces difficulties in describing the late-time cosmic acceleration and the dark sector of the Universe [10,14]. These limitations have encouraged the development of modified theories of gravity, where the standard Einstein-Hilbert action is extended to include additional geometrical or matter contributions [15–18]. Different approaches, including $f(R)$, $f(R,T)$ and teleparallel gravity, have been widely investigated in this direction [19–22].

Among these, symmetric teleparallel gravity where gravitation is described by non-metricity, the $f(Q)$ theory [23] was introduced as a natural generalization to explain cosmic acceleration without invoking dark energy [24–27]. Motivated by effective low-energy approaches to gravity and the possibility of matter–geometry interaction, this framework was further extended to $f(Q,T)$ gravity [28], where the gravitational Lagrangian is expressed as a function of both Q and the trace of the energy-momentum tensor T. The presence of the T term introduces a direct coupling between matter and geometry, which can significantly affect the cosmological dynamics and provides additional flexibility in describing the evolution of the Universe [29–31]. Consequently, $f(Q,T)$ gravity has recently attracted considerable attention as a promising modified gravity theory with significant applications in modern cosmology [32–35]. In the present work, we consider a linear form of the function given by $f(Q,T) = \alpha Q + \beta T$, and study its cosmological implications [28,36]. The field equations are solved by adopting a suitable time-dependent scale factor [37], and the resulting cosmological quantities such as energy density and pressure and equation of state parameter are obtained.

To examine the dynamical behavior of the model, we analyze the evolution of the deceleration parameter, which describes the transition from decelerated expansion to accelerated expansion of the Universe [38,39]. In addition, the equation of state parameter is studied to examine the nature of the cosmic fluid. The physical viability of the model is later investigated by analysis of energy conditions. The observational consistency of the model is tested using Markov Chain Monte Carlo (MCMC) techniques with Hubble, DESI-BAO, and Union3 datasets [40–54]. The obtained constraints are used to study the evolution of cosmological parameters and to examine the model behavior against the standard cosmological scenario.Thus, the work provides a consistent framework to study the cosmological evolution of the Universe in $f(Q,T)$ gravity [28,55] and explores its capability to describe the transition from deceleration to acceleration in agreement with observations.

This research is motivated by the aim of investigating the nature of the accelerated expansion of the Universe beyond standard dark energy paradigm. Such a framework enables the study of the combined influence of non-metricity scaler Q and the trace T of the energy–momentum tensor on the dynamical evolution of the cosmos within modified gravity theory. Thus, the $f(Q,T)$ gravity framework is adopted in the present work to investigate cosmic acceleration in the presence of matter–geometry coupling. Using observational Hubble data

Article in Press

in reconstruction methods provides an effective approach for examining the consistency of theoretical models with current cosmological observations and constraining their parameters. These investigations can improve our understanding of cosmic acceleration, structure formation, and possible modifications to General Relativity on large cosmological scales. Future applications of this research employ the use of machine learning algorithms and Bayesian statistical techniques for more accurate estimation of cosmological parameters with forthcoming observational datasets. In addition, reconstructed $f(Q,T)$ gravity models may offer valuable perspectives on dark energy behavior, gravitational physics, and the evolution of the early and late Universe.

The remainder of the paper is organized as follows. In Section 2, the basic framework of $f(Q,T)$ gravity and the corresponding field equations. Section 3 is devoted to the analysis of cosmological quantities, involving the deceleration parameter, energy density, pressure, equation of state parameter, $Om(z)$ diagnostic, and energy conditions, to study the cosmological evolution of the model. Section 4 is devoted to the observational viability of the model using different observational datasets and statistical analysis. Section 5 summarizes the results and presents a detailed discussion of the present work. And Section 6 provides the conclusions and future perspectives.

2 Framework of $f(Q,T)$ Gravity and Solution of Field Equations

The gravitational action in $f(Q,T)$ gravity defined as [28]

$$S = \frac{1}{16\pi}\int f(Q,T)\sqrt{-g}\,d^4x + \int \mathcal{L}_m\sqrt{-g}\,d^4x, \tag{2.1}$$

where Q is the non-metricity scalar, T is the trace of the energy-momentum tensor, $f(Q,T)$ is an function of Q and T, $\mathcal{L}_m$ is the matter Lagrangian density, and $g = \det(g_{\mu\nu})$.

The non-metricity scalar Q is given by [25]

$$Q = -g^{\mu\nu}(L^{\alpha}{}_{\beta\mu}L^{\beta}{}_{\nu\alpha} - L^{\alpha}{}_{\beta\alpha}L^{\beta}{}_{\mu\nu}), \tag{2.2}$$

where $L^{\alpha}{}_{\beta\gamma}$ denotes the disformation tensor

$$L^{\alpha}{}_{\beta\gamma} = -\frac{1}{2}g^{\alpha\lambda}(\nabla_{\gamma}g_{\beta\lambda} + \nabla_{\beta}g_{\gamma\lambda} - \nabla_{\lambda}g_{\beta\gamma}). \tag{2.3}$$

The traces of the non-metricity tensor are expressed as

$$Q_{\alpha} \equiv Q_{\alpha}{}^{\mu}{}_{\mu}, \qquad \tilde{Q}_{\alpha} \equiv Q^{\mu}{}_{\alpha\mu}. \tag{2.4}$$

$P^{\alpha}_{\mu\nu}$ is the superpotential tensor given by [28]

$$\begin{aligned} P^{\alpha}{}_{\mu\nu} &= \frac{1}{4}\left[-Q^{\alpha}{}_{\mu\nu} + 2Q_{(\mu}{}^{\alpha}{}_{\nu)} + Q^{\alpha}g_{\mu\nu} - \tilde{Q}^{\alpha}g_{\mu\nu} - \delta^{\alpha}_{(\mu}Q_{\nu)}\right] \\ &= -\frac{1}{2}L^{\alpha}{}_{\mu\nu} + \frac{1}{4}(Q^{\alpha} - \tilde{Q}^{\alpha})g_{\mu\nu} - \frac{1}{4}\delta^{\alpha}_{(\mu}Q_{\nu)}. \end{aligned} \tag{2.5}$$

In terms of superpotential, the nonmetricity scalar which is

$$Q = -Q_{\alpha\mu\nu}P^{\alpha\mu\nu}. \tag{2.6}$$

Article in press

In addition, the energy–momentum tensor is known to be defined as

$$T_{\mu\nu} = -\frac{2}{\sqrt{-g}}\frac{\delta(\sqrt{-g}\,\mathcal{L}_m)}{\delta g^{\mu\nu}}, \tag{2.7}$$

and

$$\Theta_{\mu\nu} = g^{\alpha\beta}\frac{\delta T_{\alpha\beta}}{\delta g^{\mu\nu}}. \tag{2.8}$$

Then the field equations by varying the gravitational action (2.1) w.r.t the components of the metric tensor are obtained as

$$8\pi T_{\mu\nu} = -\frac{2}{\sqrt{-g}}\nabla_\alpha\left(f_Q\sqrt{-g}P^\alpha_{\mu\nu}\right) - \frac{1}{2}fg_{\mu\nu} + f_T(T_{\mu\nu}+\Theta_{\mu\nu}) - f_Q\left(P_{\mu\alpha\beta}Q_\nu{}^{\alpha\beta} - 2Q^\alpha{}_{\beta\mu}P^\beta{}_{\alpha\nu}\right). \tag{2.9}$$

Now, let us assume that the Universe is described by the homogeneous, isotropic and spatially flat FLRW metric given by

$$ds^2 = -dt^2 + a^2(t)\delta_{ij}dx^i dx^j, \tag{2.10}$$

where $a(t)$ denotes the scale factor. The expansion rate is expressed in terms of the scale factor as $H = \frac{\dot{a}}{a}$. The function H represents the Hubble parameter and the non-metricity given by $Q = 6H^2$

From (2.9) and (2.10), the field equations [28] are obtained as

$$8\pi\rho = \frac{f}{2} - 6FH^2 - \frac{2\tilde{G}}{1+\tilde{G}}(\dot{F}H + F\dot{H}), \tag{2.11}$$

and

$$8\pi p = -\frac{f}{2} + 6FH^2 + 2(\dot{F}H + F\dot{H}). \tag{2.12}$$

Here, $(\cdot)$ denotes differentiation with respect to cosmic time, while $F \equiv f_Q = \partial f/\partial Q$ and $8\pi\tilde{G} \equiv f_T = \partial f/\partial T$. The relation $8\pi\tilde{G} \equiv f_T$ defines $\tilde{G}$ and does not assume f_T to be constant in the general $f(Q,T)$ framework.

Combining (2.11) and (2.12), the evolution equation for the Hubble function H takes the form

$$\dot{H} + \frac{\dot{F}H}{F} = \frac{4\pi}{F}(1+\tilde{G})(\rho+p). \tag{2.13}$$

In terms of the effective pressure and effective energy density, the field equations take the form

$$3H^2 = 8\pi\rho_{\text{eff}} = \frac{f}{4F} - \frac{4\pi}{F}\left[(1+\tilde{G})\rho + \tilde{G}p\right], \tag{2.14}$$

$$2\dot{H} + 3H^2 = -8\pi p_{\text{eff}} = \frac{f}{4F} - \frac{2\dot{F}H}{F} + \frac{4\pi}{F}\left[(1+\tilde{G})\rho + (2+\tilde{G})p\right]. \tag{2.15}$$

The effective thermodynamic quantities satisfy the following conservation equation:

$$\dot{\rho}_{\text{eff}} + 3H(\rho_{\text{eff}} + p_{\text{eff}}) = 0. \tag{2.16}$$

Article in press

3 Mathematical Formulation, cosmological evolution and Dynamical Quantities

We consider a linear $f(Q,T)$ gravity model as

$$f(Q,T) = \alpha Q + \beta T, \tag{3.1}$$

where α and β are constant parameters. For this linear form, the derivatives reduce to $f_Q = \alpha$ and $f_T = \beta$, and hence $\tilde{G} = \beta/(8\pi)$ is constant. These relations simplify the Friedmann equations (2.11) and (2.12) for our model.

The linear form is considered to keep the contributions of Q and T explicit and to study the matter–geometry coupling without introducing additional nonlinear terms. The model provides a convenient framework for cosmological evolution described by the non- metricity scaler Q and the trace of the energy momentum tensor T.

From the first field equation, we obtain the energy density.

$$\rho = \frac{\alpha \left[\beta \left(1 + \frac{3\beta}{2}\right) \dot{H} - \frac{3}{2}(2 + 5\beta + 3\beta^2)H^2\right]}{(1 + 3\beta + 2\beta^2)\left(1 + \frac{3\beta}{2}\right)}. \tag{3.2}$$

In same way, we get the pressure p from the second equation.

$$p = \frac{(1 + \frac{3\beta}{2})(2\alpha\dot{H} + 3\alpha H^2) - \frac{3\alpha\beta}{2}H^2}{1 + 3\beta + 2\beta^2}. \tag{3.3}$$

The equation of state parameter is defined as $\omega = \frac{p}{\rho}$ and it becomes

$$\omega = \frac{(1 + \frac{3\beta}{2})^2(2\dot{H} + 3H^2) - \frac{3\beta}{2}(1 + \frac{3\beta}{2})H^2}{\beta\left(1 + \frac{3\beta}{2}\right)\dot{H} - \frac{3}{2}(2 + 5\beta + 3\beta^2)H^2}. \tag{3.4}$$

The standard approach in the cosmological modeling, we consider the Hubble parameter in a parametrized form and we consider a time-dependent deceleration parameter, which is consistent with recent observational evidence indicating a transition from decelerated to accelerated expansion of the universe. The corresponding scale factor can be obtained, which helps in analyzing the evolution of the universe [56–58].

Following the standard parametrization approach, we consider a suitable form of the scale factor to describe cosmic evolution. Hence, we assume the scale factor as [56,59]

$$a(t) = (\sinh(\lambda t))^{\frac{1}{n}},$$

where λ and n are positive constants. This form is employed because it gives simple analytical expressions for the Hubble and deceleration parameters and provides a convenient description of the cosmic evolution. The corresponding Hubble parameter is given as

$$H(t) = \frac{\lambda \coth(\lambda t)}{n}.$$

To describe the cosmological evolution in terms of redshift, we use

$$1 + z = \frac{a_0}{a(t)},$$

Article in press

where a_0 is the present value of the scale factor.

The energy density is obtained as a function of cosmic time and subsequently expressed in terms of the redshift.

$$\rho(t) = \frac{\alpha\lambda^2}{(1+3\beta+2\beta^2)\left(1+\frac{3\beta}{2}\right)}\left[-\frac{\beta}{n}\left(1+\frac{3\beta}{2}\right)\operatorname{csch}^2(\lambda t) - \frac{3}{2n^2}(2+5\beta+3\beta^2)\coth^2(\lambda t)\right], \tag{3.5}$$

$$\rho(z) = -\frac{\alpha\lambda^2}{n^2(1+\beta)(1+2\beta)}\left[3(1+\beta)\left(1+(1+z)^{2n}\right)+\beta n(1+z)^{2n}\right]. \tag{3.6}$$

The pressure is determined in terms of cosmic time and then converted into redshift space.

$$p(t) = \frac{\alpha\lambda^2}{1+3\beta+2\beta^2}\left[-\frac{2}{n}(1+\frac{3\beta}{2})\operatorname{csch}^2(\lambda t) + \frac{3}{n^2}(1+\beta)\coth^2(\lambda t)\right], \tag{3.7}$$

$$p(z) = \frac{\alpha\lambda^2}{n^2(1+\beta)(1+2\beta)}\left[3(1+\beta)\left(1+(1+z)^{2n}\right) - n(2+3\beta)(1+z)^{2n}\right]. \tag{3.8}$$

Using the above expressions, we obtain the equation of state parameter, which is further obtained in terms of redshift.

$$\omega(t) = \frac{\left(1+\frac{3\beta}{2}\right)\left[-\frac{2}{n}\left(1+\frac{3\beta}{2}\right)\operatorname{csch}^2(\lambda t)+\frac{3}{n^2}(1+\beta)\coth^2(\lambda t)\right]}{\left[-\frac{\beta}{n}\left(1+\frac{3\beta}{2}\right)\operatorname{csch}^2(\lambda t) - \frac{3}{2n^2}(2+5\beta+3\beta^2)\coth^2(\lambda t)\right]}, \tag{3.9}$$

$$\omega(z) = -\frac{3(1+\beta)\left(1+(1+z)^{2n}\right) - n(2+3\beta)(1+z)^{2n}}{3(1+\beta)\left(1+(1+z)^{2n}\right)+\beta n(1+z)^{2n}}. \tag{3.10}$$

Thus, the Hubble parameter is expressed as a function of the redshift z

$$H(z) = H_0\left[\frac{1+(1+z)^{2n}}{2}\right]^{\frac{1}{2}}. \tag{3.11}$$

At the present epoch, the relation $H_0 = \sqrt{2}\lambda/n$ gives λ using the best-fit values $n = 1.315$ and $H_0 = 71.316$.

The deceleration parameter $q(z)$ is a fundamental quantity describing the expansion dynamics of the Universe. The evolution of $q(z)$ is presented in Fig. 1, where it can be seen that $q(z)$ remains positive at higher redshifts and becomes negative at lower redshifts.

The expression for the deceleration parameter is given by

$$q(z) = -1 + \frac{n(1+z)^{2n}}{1+(1+z)^{2n}}. \tag{3.12}$$

This behavior indicates a transition from an early decelerated phase to a late-time accelerated expansion. The transition redshift z_t, determined by the condition $q(z_t) = 0$, is evaluated as $z_t \approx 0.548$ for the present model, we get the constraint in the range $1 < n < 2$, which ensures the physical viability of model.The present value $q_0 < 0$ confirms that the Universe exhibits accelerated expansion at the present epoch.

For the graphical analysis, we fix $\alpha = -1$ and use the observationally constrained value $n = 1.315$. In the convention adopted in this work, the uncoupled limit $\beta = 0$ gives $8\pi\rho = -3\alpha H^2$. Therefore, $\alpha = -1$ recovers the standard first Friedmann equation. For the

Article in press

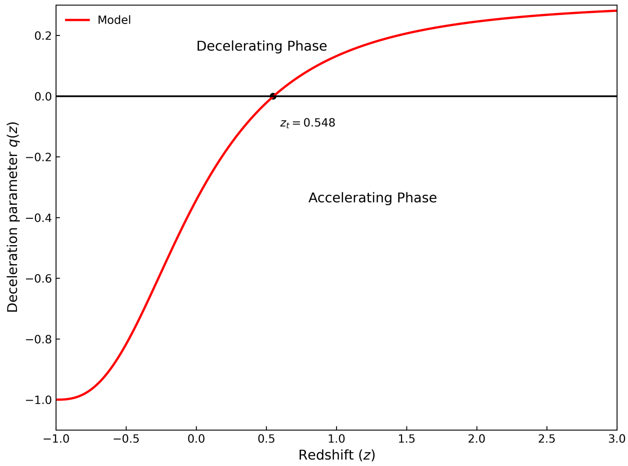

Figure 1: Evolution of the deceleration parameter $q(z)$ versus Redshift z

present value of n, the positive coupling branch begins close to the critical value $\beta_c \simeq 0.392$, associated with an approximately matter-like high-redshift behaviour. Thus, we use the representative values $\beta = 0.40$, 1.00, and 2.00 to examine the influence of the matter–geometry coupling on the cosmological evolution. The same set of parameters is used consistently in the following physical analysis.

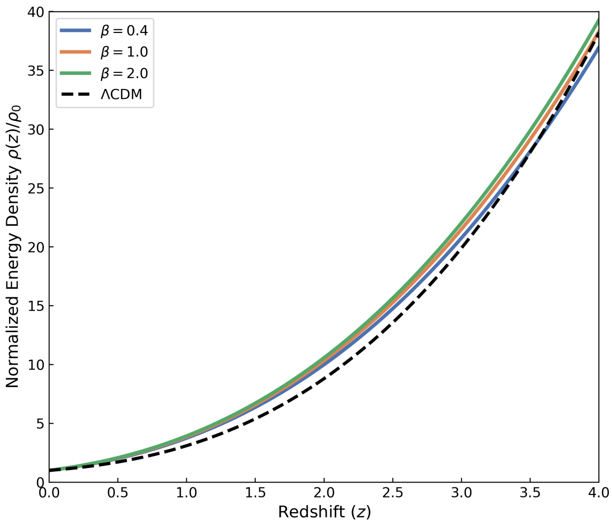

Figure 2: Evolution of the normalized energy density $\rho(z)/\rho_0$ with redshift z for $\alpha = -1$ and different representative values of β.

The evolution of the normalized energy density $\rho(z)/\rho_0$ is shown in Fig. 2 for different representative values of the coupling parameter β. The normalized energy density remains positive throughout the considered redshift range and increases monotonically with z, indicating a larger energy density at earlier epochs.The three curves follow nearly the same

Article in press

evolutionary pattern, although a slight increase in $\rho(z)/\rho_0$ is observed for larger values of β. This shows that the energy-density evolution is only mildly sensitive to the matter–geometry coupling in the considered parameter range. Compared with the ΛCDM curve, the present model exhibits a similar overall growth with redshift, with a modest deviation becoming visible at higher z. Such deviations from the standard cosmological evolution are relevant when examining dynamical alternatives to the cosmological-constant scenario [60,61].

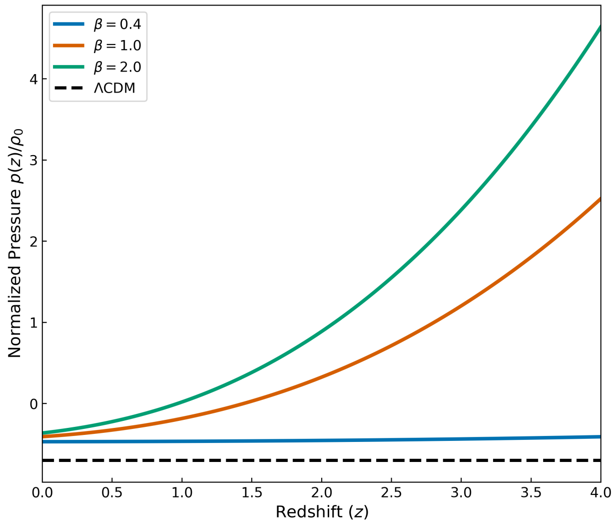

Figure 3: Evolution of the normalized pressure $p(z)/\rho_0$ with redshift z for $\alpha = -1$ and different representative values of β.

As illustrated in Fig. 3, the normalized pressure $p(z)/\rho_0$ shows a noticeable dependence on the coupling parameter β. For larger values of β, the pressure is positive at higher redshift and crosses the zero-pressure line during the cosmic evolution, becoming negative towards the present epoch. In contrast, the lower-β case remains negative and shows a comparatively mild variation. Thus, the pressure evolves towards more negative values as the redshift decreases, indicating that the negative-pressure contribution becomes important at late times. This behaviour is consistent with the accelerated phase of cosmic evolution [62]. The dashed ΛCDM curve is included as a reference for comparison with the dynamical pressure predicted by the present model.

Figure 4 presents the behaviour of the equation-of-state parameter $\omega(z)$ for different representative values of β. At higher redshift, $\omega(z)$ remains close to zero, showing an approximately matter-like behaviour. As the Universe evolves towards the present epoch, $\omega(z)$ becomes more negative and enters the range $-1 < \omega < -1/3$, indicating a quintessence-like regime [63,64].The coupling parameter β affects the magnitude of $\omega(z)$, with larger values of β giving comparatively less negative values of the equation of state. This late-time negative-pressure behaviour is consistent with the accelerating phase obtained from the background evolution.

Article in Press

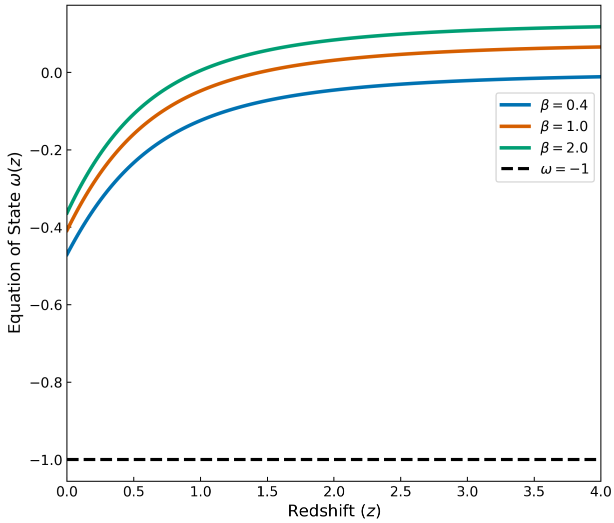

Figure 4: Evolution of the equation-of-state parameter $\omega(z)$ with redshift z for $\alpha = -1$ and different representative values of β. The dashed line denotes the cosmological-constant limit $\omega = -1$.

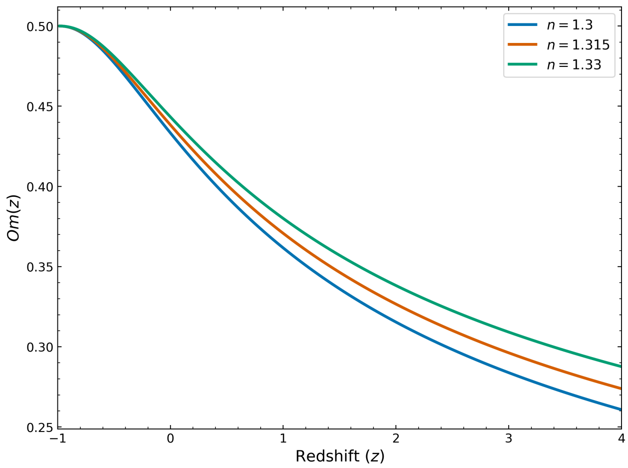

Figure 5: Evolution of the $Om(z)$ diagnostic with redshift z for $n = 1.30$, 1.315, and 1.33, where $n = 1.315$ represents the best-fit value.

3.1 Model Discrimination via the $Om(z)$ Diagnostic

The $Om(z)$ diagnostic [65,66] provides a useful geometrical test of the cosmic expansion history and is defined as

$$Om(z) = \frac{E^2(z) - 1}{(1+z)^3 - 1}, \tag{3.13}$$

where $E(z) = H(z)/H_0$. For the ΛCDM model, $Om(z)$ remains constant with redshift, whereas its variation can distinguish different dark-energy behaviours. A decreasing $Om(z)$

Article in Press

with increasing redshift is associated with a quintessence-like evolution [67], while an increasing trend corresponds to a phantom-like behaviour.

For the present model, Fig. 5 presents the $Om(z)$ diagnostic for the best-fit value $n = 1.315$ together with the representative neighbouring values $n = 1.30$ and 1.33. All three trajectories decrease smoothly as the redshift increases, indicating a quintessence-like cosmological behaviour. The same qualitative trend is preserved around the best-fit value, showing that this behaviour is not restricted to a single choice of n. Moreover, larger values of n shift the $Om(z)$ trajectory towards higher values, reflecting the sensitivity of the expansion history to the model parameter.

3.2 Analysis of Energy Conditions

Energy conditions provide an important test of the physical behaviour of cosmological models and are widely used to examine different phases of cosmic evolution in modified gravity [68,69].For the analysis presented in Fig. 6, we fix $\alpha = -1$ and consider the representative coupling value $\beta = 1$, while the remaining parameters are taken from their adopted best-fit values.

From Fig. 6, the quantities $\rho + p$ and $\rho - p$ remain positive over the entire redshift range, indicating that the NEC and DEC are satisfied, while the positive energy density also supports the WEC. The main feature is observed in $\rho + 3p$, which changes sign near the present epoch and becomes negative below approximately $z \simeq 0.11$. This indicates the violation of the SEC in the late-time region, consistent with the accelerated phase of cosmic evolution [70]. This result also agrees with the quintessence-like behavior obtained from the equation of state.

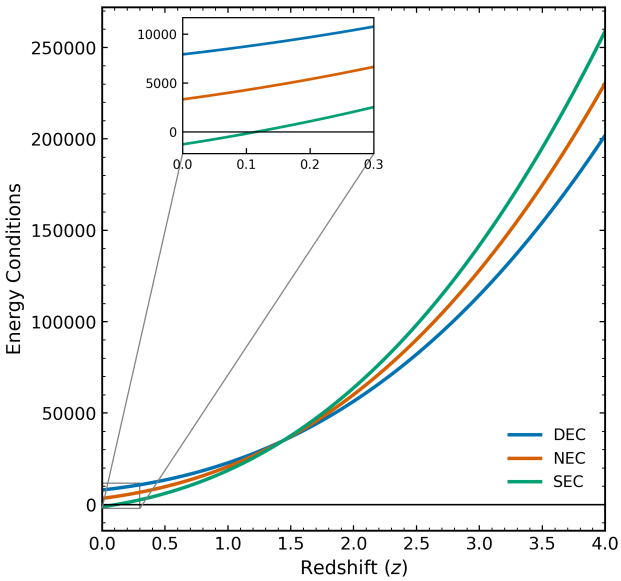

Figure 6: Redshift evolution of the null, dominant, and strong energy conditions for $\alpha = -1$ and the representative coupling value $\beta = 1$.

Article in press

4 Observational Viability of the Model

Hubble Dataset

In this present work, we make use of the observational Hubble parameter data, which provide information about the expansion rate of the Universe across various redshifts. The data set consists of 30 data points that cover the redshift range $0.07 \leq z \leq 1.965$. These measurements are mainly obtained using the differential age cosmic chronometer method, where the expansion rate is determined from the variation of redshift with cosmic time [71–76].

The Hubble function H(z) is defined as

$$H(z) = -\frac{1}{1+z}\frac{dz}{dt}. \tag{4.1}$$

To compare the theoretical model with observations, we use the standard chi-square minimization technique given by [77]

$$\chi_H^2 = \sum_{i=1}^{30} \frac{\left[H_{\rm th}(z_i) - H_{\rm obs}(z_i)\right]^2}{\sigma^2_{H(z_i)}}, \tag{4.2}$$

where $H_{\rm th}$, $H_{\rm obs}$, and $\sigma_{H(z_i)}$ represent the theoretical value, observed value, and the corresponding uncertainty of the Hubble parameter, respectively. The $H(z)$ data points used in this work are listed in Table 1.

Table 1: Compilation of observational measurements of the Hubble parameter $H(z)$.

z	$H(z)$	σ_H	Ref.	z	$H(z)$	σ_H	Ref.
0.070	69	19.6	[78]	0.4783	80.9	9	[81]
0.090	69	12	[79]	0.480	97	62	[82]
0.120	68.6	26.2	[78]	0.593	104	13	[80]
0.170	83	8	[79]	0.6797	92	8	[80]
0.1791	75	4	[80]	0.7812	105	12	[80]
0.1993	75	5	[80]	0.8754	125	17	[80]
0.200	72.09	29.6	[78]	0.880	90	40	[82]
0.270	77	14	[79]	0.900	117	23	[79]
0.280	88.8	36.6	[78]	1.037	154	20	[80]
0.3519	83	14	[80]	1.300	168	17	[79]
0.400	95	17	[79]	1.363	160	33.6	[83]
0.4004	77	10.2	[81]	1.430	177	18	[79]
0.4247	87.1	11.2	[81]	1.530	140	14	[79]
0.4497	92.8	12.9	[81]	1.750	202	40	[79]
0.3802	83	13.5	[81]	1.965	186.5	50.4	[83]

DESI BAO Datasets

We use the DESI Year-1 BAO dataset which contains 12 data points obtained from multiple tracers, including Bright Galaxy Samples (BGS), Luminous Red Galaxies (LRGs), Emission Line Galaxies (ELGs), and quasars (QSO), and dataset covers the redshift range $0.295 \leq z \leq 2.33$ [84–87].

Article in press

The BAO observations provide geometrical constraints through the scaled distance quantities $D_M(z)/r_d$, $D_H(z)/r_d$, and $D_V(z)/r_d$, where r_d denotes the sound horizon at the drag epoch [88].

Here, $D_H(z)$ is the Hubble distance and $D_M(z)$ denotes the transverse comoving distance,

$$D_M(z) \equiv c \int_0^z \frac{dz'}{H(z')}, \quad D_H(z) \equiv \frac{c}{H(z)}, \tag{4.3}$$

The volume-averaged distance $D_V(z)$ is defined as

$$D_V(z) \equiv \left[z\, D_M^2(z)\, D_H(z)\right]^{1/3}. \tag{4.4}$$

Table 2: DESI BAO measurements across different redshift values.

Redshift z	Observable	Tracer	Measured Value
0.295	D_V/r_d	BGS	7.93
0.51	D_M/r_d	LRG1	13.62
0.51	D_H/r_d	LRG1	20.98
0.71	D_M/r_d	LRG2	16.85
0.71	D_H/r_d	LRG2	20.08
0.93	D_M/r_d	LRG3+ELG1	21.71
0.93	D_H/r_d	LRG3+ELG1	17.88
1.32	D_M/r_d	ELG2	27.79
1.32	D_H/r_d	ELG2	13.82
1.49	D_V/r_d	QSO	26.07
2.33	D_M/r_d	Lyα QSO	39.71
2.33	D_H/r_d	Lyα QSO	8.52

Union 3 Datasets

We use Type Ia supernova data from the Union 3 compilation Type Ia supernovae are well established standard candles and are widely used to study the expansion history of the Universe [89–91]. The full Union3 sample contains a large number of supernova observations. However, for the present analysis, we consider a subset of 22 data points covering the redshift range $0.05 \leq z \leq 2.26$.

The observable quantity is the distance modulus, defined as

$$\mu(z) = m - M = 25 + 5\log_{10}\left(\frac{d_L(z)}{\text{Mpc}}\right), \tag{4.5}$$

The luminosity distance $d_L(z)$ is given by

$$d_L(z) = c\,(1+z)\int_0^z \frac{dz'}{H(z')}. \tag{4.6}$$

These observational data are utilized to constrain the cosmological model through comparison with the theoretical predictions.

Fig 7 displays the MCMC Marginalized distributions and confidence regions for the parameters H_0 and n inferred from the Hubble dataset. The corresponding MCMC contour analysis for the combined Hubble+DESI BAO dataset is presented in Fig 9, while Fig 11

Article in press

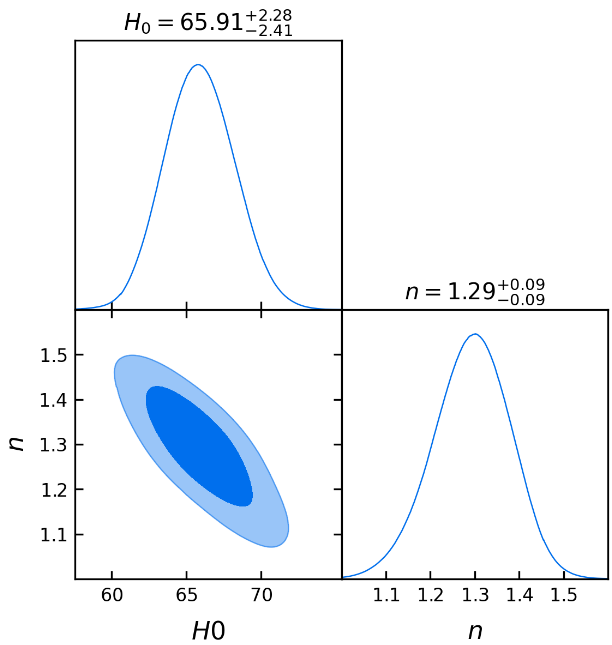

Figure 7: Marginalized distributions and confidence regions for the parameters H_0 and n inferred from the Hubble dataset

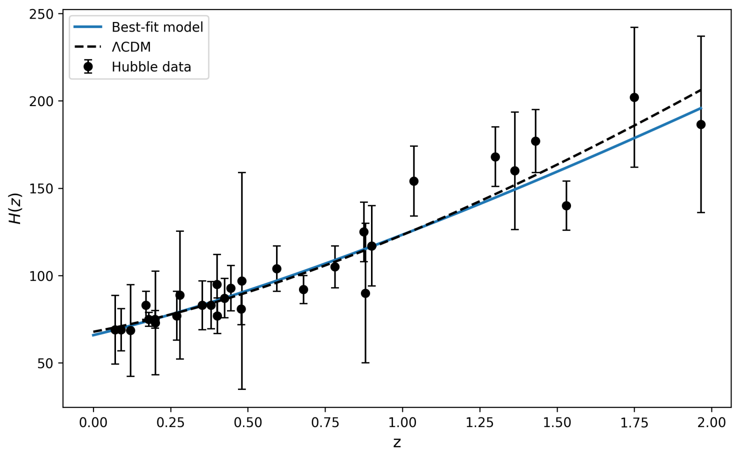

Figure 8: Observational H(z) measurements with error bars together with the ΛCDM model.

illustrates the MCMC posterior behavior for the combined Hubble+DESI BAO+Union3 observational dataset. The off–diagonal panels represent the two–dimensional confidence contours between the model parameters, whereas the diagonal panels denote the associated one-dimensional marginalized distributions obtained from the Markov Chain Monte Carlo (MCMC) analysis. In these contour plots, the darker inner shaded regions correspond to the 1σ (68%) confidence level, indicating the region most consistent with the observational data, while the lighter outer shaded regions denote the 2σ (95%) confidence level with com-

Article in Press

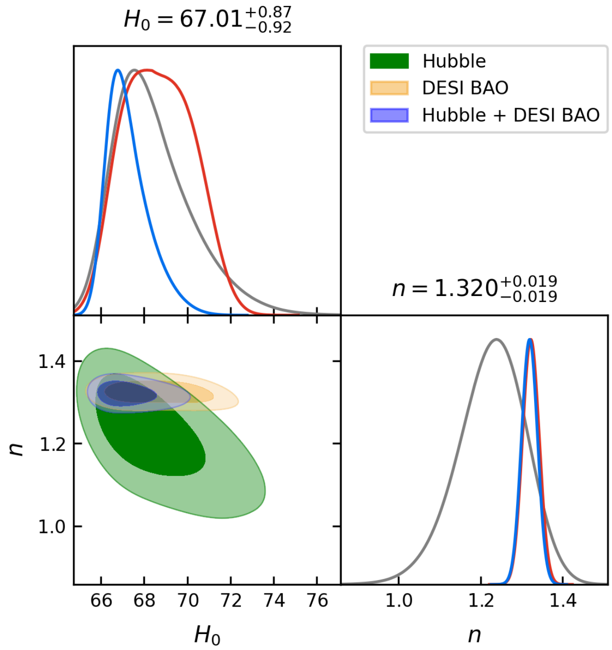

Figure 9: Confidence regions and posterior distributions corresponding to the parameters H_0 and n constrained by the Hubble, DESI BAO and Combined datasets.

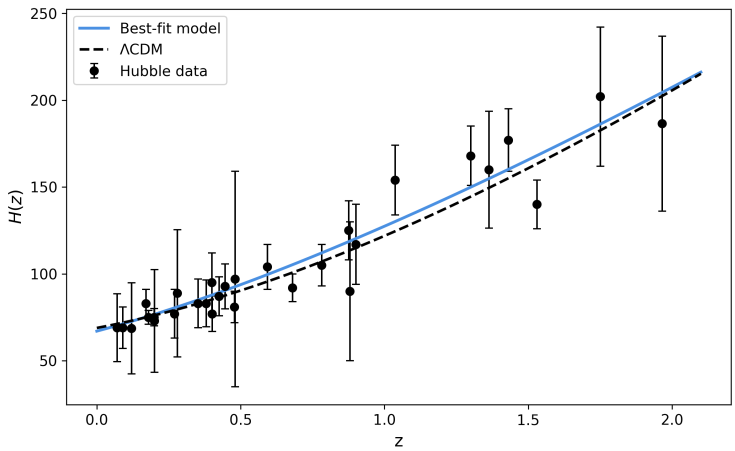

Figure 10: Combined Hubble + DESI BAO observational data with error bars compared with ΛCDM model

paratively broader parameter uncertainties. It can be clearly noticed that the inclusion of additional observational datasets leads to progressively tighter and more compact confidence contours, reflecting improved constraints on the cosmological parameters H_0 and n. In particular, the combined Hubble+DESI BAO+Union3 dataset provides more restricted bounds on the parameters compared to the individual datasets, indicating improved precision and

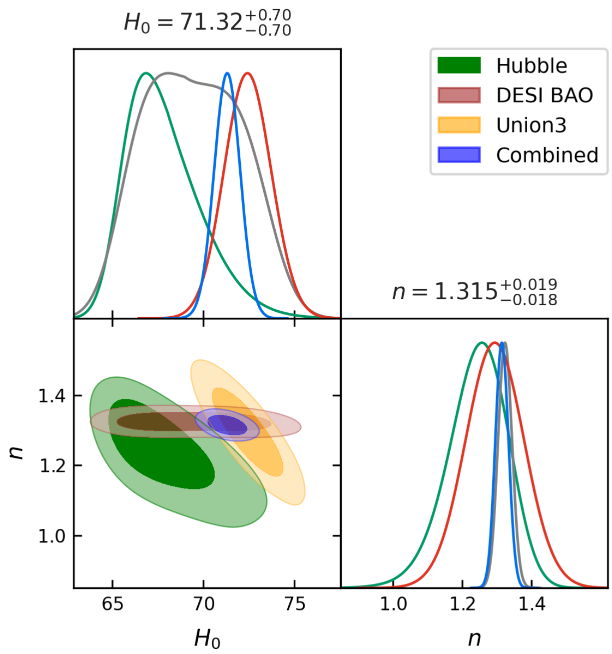

Figure 11: Confidence regions and marginalized distributions for the parameters H_0 and n derived from the Hubble, DESI BAO, Union3 and Combined datasets

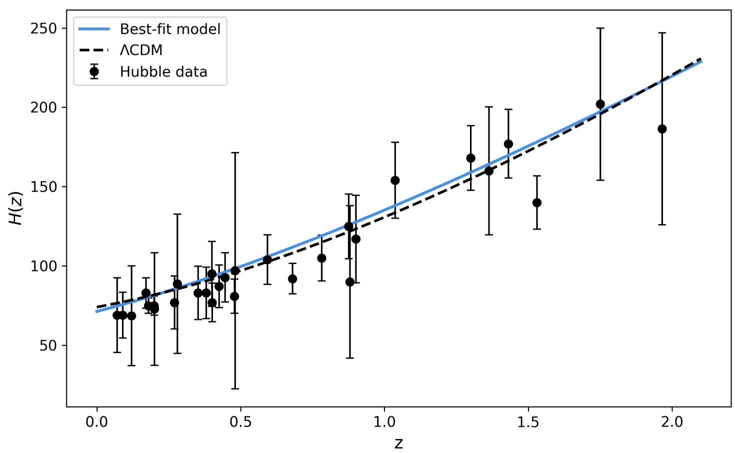

Figure 12: Combined Hubble + DESI BAO + Union3 observational data compared with the ΛCDM model

stability of the obtained cosmological results. Moreover, the overlap and smooth behavior of the posterior distributions indicate a well-converged MCMC analysis and support the consistency of the obtained parameter estimations with recent cosmological observations.

Fig 8 shows the comparison of the Hubble parameter $H(z)$ with the observational Hubble data and the ΛCDM model. The blue curve represents the best-fit behavior of the present

Table 3: Best-fit parameter estimates and associated 1σ confidence limits obtained from observational data.

Data used	Parameters	Best fit values
Hubble	H_0	$65.911^{+2.280}_{-2.409}$
	n	$1.294^{+0.088}_{-0.085}$
Hubble + DESI BAO	H_0	$67.009^{+0.540}_{-0.997}$
	n	$1.320^{+0.019}_{-0.019}$
	r_d	$143.548^{+2.460}_{-2.068}$
Hubble+DESI BAO+Union3	H_0	$71.316^{+0.697}_{-0.701}$
	n	$1.315^{+0.019}_{-0.018}$
	r_d	$135.330^{+1.570}_{-1.526}$

Table 4: Statistical estimators of the model derived from various observational datasets.

Data used	χ^2	Red χ^2	AIC	BIC	ΔAIC	ΔBIC
Hubble	14.943	0.534	18.943	21.746	0.402	0.402
Hubble + DESI BAO	31.757	0.814	37.75	42.97	7.484	7.484
Hubble+DESI BAO+Union3	47.116	0.772	53.11	59.59	9.943	9.943

model, while the black dashed curve denotes the prediction ΛCDM. It is observed that the Hubble parameter increases smoothly with redshift, illustrating the expansion behavior of the Universe at distinct cosmic epochs. The model follows the observational trend quite well and remains close to the ΛCDM curve over most of the redshift region, showing good agreement with the available Hubble observations.

Fig 10 displays the comparison of the combined Hubble+ DESIBAO observational data with the ΛCDM model. It can be observed that the Hubble parameter increases continuously with increasing redshift, reflecting the continuous expansion of the Universe over distinct stages of cosmic evolution. The obtained model remains close to prediction throughout ΛCDM for the redshift region considered and a reliable and physically consistent description of the current cosmological observations. Fig 12 establishes the comparison between the combined Hubble+ DESIBAO +Union3 observational data set and the ΛCDM model. It can be noticed that the Hubble parameter increases steadily with redshift, depicting the expansion pattern of the Universe over different cosmological periods and seen that the best-fit model obtained remains very close to the ΛCDM behavior throughout the redshift interval and follows the observational data points with good accuracy. This implies that the present analysis exhibits strong consistency with current observational evidence and supports the viability of the proposed cosmological model.

Table 3 presents the best-fit parameter estimates together with their corresponding 1σ confidence intervals of H_0 and n derived from the Hubble, Hubble+DESIBAO, and Hubble+DESIBAO+Union3 observational datasets through the MCMC analysis. These observationally constrained parameter values are used in subsequent cosmological analysis and graphical investigations discussed in the present work. Table 4 summarizes the statistical estimators of the present cosmological model for different observational datasets. The values of χ^2, Red χ^2, AIC, BIC, ΔAIC, and ΔBIC are used to examine the statistical performance and observational compatibility of the model.

Article in Press

5 Results and Discussion

The model parameters are constrained using the Hubble, DESI BAO, and Union3 datasets, both individually and in combination. For the Hubble dataset alone, the MCMC analysis gives $H_0 = 65.911^{+2.280}_{-2.409}\,\mathrm{km\,s^{-1}\,Mpc^{-1}}$, $n = 1.294^{+0.088}_{-0.085}$. The reduced chi-square, $\chi^2_{\mathrm{red}} = 0.534$, indicates a satisfactory fit, with $\Delta\mathrm{AIC} = \Delta\mathrm{BIC} = 0.402$. For the combined Hubble+DESI BAO analysis, the constraints become significantly tighter, yielding $H_0 = 67.009^{+0.540}_{-0.997}\,\mathrm{km\,s^{-1}\,Mpc^{-1}}$, $n = 1.320^{+0.019}_{-0.019}$, and $r_d = 143.548^{+2.460}_{-2.068}\,\mathrm{Mpc}$. The substantial reduction in the parameter uncertainties, particularly for n, highlights the complementary constraining power of the DESI BAO data. The corresponding $\chi^2_{\mathrm{red}} = 0.814$, with $\Delta\mathrm{AIC} = \Delta\mathrm{BIC} = 7.484$, indicates a satisfactory fit while providing a useful comparison with the reference model. With the further inclusion of the Union3 dataset, the combined analysis gives $H_0 = 71.316^{+0.697}_{-0.701}\,\mathrm{km\,s^{-1}\,Mpc^{-1}}$, $n = 1.315^{+0.019}_{-0.018}$, and $r_d = 135.330^{+1.570}_{-1.526}\,\mathrm{Mpc}$. The parameter n remains tightly constrained, while the uncertainty in H_0 is also substantially reduced compared with the Hubble-only analysis [92]. The resulting $\chi^2_{\mathrm{red}} = 0.772$ indicates a good overall fit, whereas $\Delta\mathrm{AIC} = 9.943$ and $\Delta\mathrm{BIC} = 9.943$ indicate a stronger statistical preference for the reference model.

Overall, the results demonstrate the importance of combining complementary observational probes. The joint analyses substantially improve the precision of the parameter constraints and reduce degeneracies compared with the Hubble-only analysis. At the same time, the increasing ΔAIC and ΔBIC values indicate that, although the proposed model provides a satisfactory fit to the observations, the reference model remains statistically favored in the model-comparison analysis. The present work provides an observationally constrained framework for exploring holographic dark energy in f(Q,T) gravity, where the reconstructed Hubble parameter offers a natural geometric basis for implementing holographic prescriptions. The stable constraints from the combined Hubble+DESI BAO+Union3 analysis demonstrate observationally viable cosmic dynamics, thereby supporting the potential of the reconstructed $f(Q,T)$ framework for studying holographic descriptions of the dark sector.

From the analysis of cosmological evolution, the deceleration parameter $q(z)$ exhibits a clear transition from positive to negative values, indicating a shift from an early decelerated phase to a late-time accelerated expansion. This behavior is in good agreement with current observational evidence.

The normalized energy density increases with redshift and shows only a mild dependence on the coupling parameter β, with a modest deviation from the ΛCDM behaviour at higher redshifts. The normalized pressure evolves towards more negative values as the Universe approaches the present epoch; for larger β, it changes from positive values at higher redshift to negative values at late times. The equation-of-state evolution indicates a transition from an approximately matter-like state at higher redshift to a quintessence-like regime near the present epoch. Consistently, the decreasing $Om(z)$ trajectories, including the best-fit case $n = 1.315$, support the same quintessence-like behaviour. Thus, both diagnostics provide a consistent picture of the late-time evolution of the model.

Such persistent phantom-like behavior, $\omega(z) < -1$, and negative effective pressure are qualitatively consistent with holographic dark-energy scenarios, providing a useful basis for comparing the reconstructed $f(Q,T)$ cosmology with holographic descriptions of late-time cosmic acceleration.

The energy-condition analysis shows that the null, weak, and dominant energy conditions are satisfied, while the strong energy condition is violated at late times. The quintessence-like evolution obtained in the model. Overall, the observational and cosmological results

Article in press

show that the proposed model consistently describes the late-time accelerated evolution of the Universe.

6 Conclusion

In this work, we have investigated the cosmological implications of the $f(Q,T) = \alpha Q + \beta T$ gravity model using observational datasets including Hubble, DESIBAO, and Union3. The model parameters were constrained through MCMC analysis, providing reliable estimates consistent with observational data. The cosmological analysis shows that the deceleration parameter indicates a transition from early-time deceleration to late-time acceleration, consistent with observational evidence. The equation-of-state parameter evolves from an approximately matter-like behaviour at higher redshift to the quintessence-like region, $-1 < \omega < -1/3$, towards the present epoch. The energy-condition analysis shows that the NEC, WEC, and DEC remain satisfied, whereas the SEC is violated at late times. It is concluded that the proposed model provides a consistent description of cosmic evolution and offers a viable framework for explaining the present accelerated phase of the Universe.

The results indicate that the proposed framework remains compatible with observational data, with a slight deviation from the ΛCDM model. Hence, this research develops viable reconstructed cosmological models within the framework of $f(Q,T)$ gravity that accurately fit observational Hubble parameter measurements and effectively explain the observed expansion behavior of the Universe.

Authors' Contributions

A. M. conceptualized the study and wrote the initial draft; P. K. D. carried out the analytical calculations; A. M. and R.P. performed numerical simulations and data analysis; and S. I. supervised the research and contributed to manuscript revision. All authors reviewed and approved the final version of the manuscript.

Data Availability

The manuscript has no associated data or the data will not be deposited.

Conflicts of Interest

The authors declare that there is no conflict of interest.

Ethical Considerations

The authors have diligently addressed ethical concerns, such as informed consent, plagiarism, data fabrication, misconduct, falsification, double publication, redundancy, submission, and other related matters.

Article in press

Funding

This research did not receive any grant from funding agencies in the public, commercial, or non-profit sectors.

Acknowledgements

PKD wish to mention that the part of the numerical computation of this work was carried out on the Pegasus Computing Cluster of IUCAA, Pune, India and also acknowledges the Inter-University Centre for Astronomy and Astrophysics (IUCAA), Pune, India, for providing him a Visiting Associateship under which a part of this work was carried out.

References

[1] A. G. Riess, A. V. Filippenko, P. Challis, A. Clocchiatti, A. Diercks, P. M. Garnavich, *et al.*, "Observational evidence from supernovae for an accelerating universe and a cosmological constant," Astron. J. **116**(3), 1009 (1998). DOI: 10.1086/300499.

[2] S. Perlmutter, G. Aldering, G. Goldhaber, R. A. Knop, P. Nugent, P. G. Castro, *et al.*, "Measurements of Ω and Λ from 42 high-redshift supernovae," Astrophys. J. **517**(2), 565 (1999). DOI: 10.1086/307221.

[3] S. Weinberg, Cosmology (OUP Oxford, 2008).

[4] A. G. Riess, L. G. Strolger, J. Tonry, S. Casertano, H. C. Ferguson, B. Mobasher, *et al.*, "Type Ia supernova discoveries at z> 1 from the Hubble Space Telescope: Evidence for past deceleration and constraints on dark energy evolution," Astrophys. J. **607**(2), 665 (2004). DOI: 10.1086/383612.

[5] E. Komatsu, J. Dunkley, M. R. Nolta, C. L. Bennett, B. Gold, G. Hinshaw, *et al.*, "Five-year wilkinson microwave anisotropy probe observations: cosmological interpretation," Astrophys. J. Suppl. Ser. **180**(2), 330 (2009). DOI: 10.1088/0067-0049/180/2/330.

[6] Z. Y. Huang, B. Wang, E. Abdalla and R. K. Su, "Holographic explanation of wide-angle power correlation suppression in the cosmic microwave background radiation," J. Cosmol. Astropart. Phys. **2006**(05), 013 (2006). DOI: 10.1088/1475-7516/2006/05/013.

[7] D. J. Eisenstein, I. Zehavi, D. W. Hogg, R. Scoccimarro, M. R. Blanton, R. C. Nichol, *et al.*, "Detection of the baryon acoustic peak in the large-scale correlation function of SDSS luminous red galaxies," Astrophys. J. **633**(2), 560 (2005). DOI: 10.1086/466512.

[8] L. Anderson, E. Aubourg, S. Bailey, F. Beutler, V. Bhardwaj, M. Blanton, *et al.*, "The clustering of galaxies in the SDSS-III Baryon Oscillation Spectroscopic Survey: baryon acoustic oscillations in the Data Releases 10 and 11 Galaxy samples," Mon. Not. R. Astron. Soc. **441**(1), 24 (2014). DOI: 10.1093/mnras/stu523.

[9] E. J. Copeland, M. Sami and S. Tsujikawa, "Dynamics of dark energy," Int. J. Mod. Phys. D **15**(11), 1753 (2006). DOI: 10.1142/S021827180600942X.

[10] E. Komatsu, J. Dunkley, M. R. Nolta, C. L. Bennett, B. Gold, G. Hinshaw, *et al.*, "Five-year wilkinson microwave anisotropy probe observations: cosmological interpretation," Astrophys. J. Suppl. Ser. **180**(2), 330 (2009). DOI: 10.1088/0067-0049/180/2/330.

Article in press

[11] R. R. Caldwell and M. Kamionkowski, "The physics of cosmic acceleration," Annu. Rev. Nucl. Part. Sci. **59**, 397 (2009). DOI: 10.1146/annurev-nucl-010709-151330.

[12] D. N. Spergel, L. Verde, H. V. Peiris, E. Komatsu, M. R. Nolta, C. L. Bennett, *et al.*, "First-year Wilkinson Microwave Anisotropy Probe (WMAP) observations: determination of cosmological parameters," Astrophys. J. Suppl. Ser. **148**(1), 175 (2003). DOI: 10.1086/377226.

[13] M. Chevallier and D. Polarski, "Accelerating universes with scaling dark matter," Int. J. Mod. Phys. D **10**(02), 213 (2001). DOI: 10.1142/S0218271801000822.

[14] S. I. Nojiri, S. D. Odintsov and D. Sáez-Gómez, "Cosmological reconstruction of realistic modified F (R) gravities," Phys. Lett. B **681**(1), 74 (2009). DOI: 10.1016/j.physletb.2009.09.045.

[15] A. Einstein, "The general theory of relativity," in The meaning of relativity, pp. 54-75 (Springer Netherlands, Dordrecht, 1922).

[16] T. Clifton, P. G. Ferreira, A. Padilla and C. Skordis, "Modified gravity and cosmology," Phys. Rep. **513**(1-3), 1 (2012). DOI: 10.1016/j.physrep.2012.01.001.

[17] S. Capozziello and M. Francaviglia, "Extended theories of gravity and their cosmological and astrophysical applications," Gen. Relativ. Gravit. **40**(2), 357 (2008). DOI: 10.1007/s10714-007-0551-y.

[18] S. Capozziello and M. De Laurentis, "Extended theories of gravity," Phys. Rep. **509**(4-5), 167 (2011). DOI: 10.1016/j.physrep.2011.09.003.

[19] H. A. Buchdahl, "Non-linear Lagrangians and cosmological theory," Mon. Not. R. Astron. Soc. **150**(1), 1 (1970). DOI: 10.1093/mnras/150.1.1.

[20] T. P. Sotiriou and V. Faraoni, "f (R) theories of gravity," Rev. Mod. Phys. **82**(1), 451 (2010). DOI: 10.1103/RevModPhys.82.451.

[21] T. Harko, F. S. Lobo, S. I. Nojiri and S. D. Odintsov, "f (R, T) gravity," Phys. Rev. D **84**(2), 024020 (2011). DOI: 10.1103/PhysRevD.84.024020.

[22] R. Aldrovandi and J. G. Pereira, Teleparallel gravity: an introduction, Vol. 173 (Springer Science & Business Media, 2012).

[23] T. Harko, T. S. Koivisto, F. S. Lobo, G. J. Olmo and D. Rubiera-Garcia, "Coupling matter in modified Q gravity," Phys. Rev. D **98**(8), 084043 (2018). DOI: 10.1103/PhysRevD.98.084043.

[24] J. B. Jiménez, L. Heisenberg and T. S. Koivisto, "Teleparallel palatini theories," J. Cosmol. Astropart. Phys. **2018**(08), 039 (2018). DOI: 10.1088/1475-7516/2018/08/039.

[25] J. B. Jiménez, L. Heisenberg and T. Koivisto, "Coincident general relativity," Phys. Rev. D **98**(4), 044048 (2018). DOI: 10.1103/PhysRevD.98.044048.

[26] R. Lazkoz, F. S. Lobo, M. Ortiz-Baños and V. Salzano, "Observational constraints of f (Q) gravity," Phys. Rev. D **100**(10), 104027 (2019). DOI: 10.1103/PhysRevD.100.104027.

Article in press

Article in press

[27] S. I. Nojiri and S. D. Odintsov, "Unified cosmic history in modified gravity: from F (R) theory to Lorentz non-invariant models," Phys. Rep. **505**(2-4), 59 (2011). DOI: 10.1016/j.physrep.2011.04.001.

[28] Y. Xu, G. Li, T. Harko and S. D. Liang, "f (Q, T) gravity," Eur. Phys. J. C **79**(8), 708 (2019). DOI: 10.1140/epjc/s10052-019-7207-4.

[29] N. Godani and G. C. Samanta, "FRW cosmology in f (Q, T) gravity," Int. J. Geom. Methods Mod. Phys. **18**(09), 2150134 (2021). DOI: 10.1142/S0219887821501346.

[30] S. Arora, S. K. J. Pacif, S. Bhattacharjee and P. K. Sahoo, "f (Q, T) gravity models with observational constraints," Phys. Dark Universe **30**, 100664 (2020). DOI: 10.1016/j.dark.2020.100664.

[31] S. Arora, A. Parida and P. K. Sahoo, "Constraining effective equation of state in f (Q, T) gravity," Eur. Phys. J. C **81**(6), 555 (2021). DOI: 10.1140/epjc/s10052-021-09358-4.

[32] S. Arora and P. K. Sahoo, "Energy conditions in f (Q, T) gravity," Phys. Scr. **95**(9), 095003 (2020). DOI: 10.1088/1402-4896/abaddc.

[33] M. Koussour, N. Myrzakulov, S. H. Shekh and M. Bennai, "Quintessence Universe and cosmic acceleration in f (Q, T) gravity," Int. J. Mod. Phys. D **31**(16), 2250115 (2022). DOI: 10.1142/S0218271822501152.

[34] S. A. Narawade, M. Koussour and B. Mishra, "Constrained f (Q, T) gravity accelerating cosmological model and its dynamical system analysis," Nucl. Phys. B **992**, 116233 (2023). DOI: 10.1016/j.nuclphysb.2023.116233.

[35] S. Rathore, S. S. Singh, S. Muhammad and E. E. Zotos, "Phase space properties of cosmological models in f (Q, T) gravity," Eur. Phys. J. C **84**(10), 1108 (2024). DOI: 10.1140/epjc/s10052-024-13464-4.

[36] R. Bhagat, S. V. Lohakare and B. Mishra, "Exploring the viability of f (Q, T) gravity: Constraining parameters with cosmological observations," Phys. Dark Universe 102048 (2025). DOI: 10.1016/j.dark.2025.102048.

[37] C. Chawla, R. K. Mishra and A. Pradhan, "String cosmological models from early deceleration to current acceleration phase with varying G and," Eur. Phys. J. Plus **127**(11), 137 (2012). DOI: 10.1140/epjp/i2012-12137-4.

[38] O. Farooq and B. Ratra, "Hubble parameter measurement constraints on the cosmological deceleration–acceleration transition redshift," Astrophys. J. Lett. **766**(1), L7 (2013). DOI: 10.1088/2041-8205/766/1/L7.

[39] J. V. Cunha and J. A. S. D. Lima, "Transition redshift: new kinematic constraints from supernovae," Mon. Not. R. Astron. Soc. **390**(1), 210 (2008). DOI: 10.1111/j.1365-2966.2008.13640.x.

[40] P. K. Dhankar, M. Albert, M. Thakre, S. Islam, F. Rahaman and B. Pourhassan, "Observational Constraints on Scalar Field Covariant Perturbations in Modified Gauss–Bonnet Gravity," Phys. Lett. B 140485 (2026). DOI: 10.1016/j.physletb.2026.140485.

[41] P. K. Dhankar, D. Mhamdi, A. Munyeshyaka, D. Kumar, J. Ntahompagaze and T. Ouali, "Testing Gauss–Bonnet gravity with DESI BAO data," Eur. Phys. J. C **86**(4), 355 (2026). DOI: 10.1140/epjc/s10052-026-15607-1.

[42] M. Thakre, P. K. Dhankar, S. Islam, P. Sahoo, F. Rahaman and B. Pourhassan, “A Bayesian Statistical Study of Bianchi Type-I Universe in $f(R, T^{\psi})$ Modified Gravity,” arXiv preprint arXiv:2601.03116 (2026). DOI: 10.48550/arXiv.2601.03116.

[43] A. Munyeshyaka, P. K. Dhankar and J. Ntahompagaze, “Perturbations with bulk viscosity in modified chaplygin gas cosmology,” Int. J. Geom. Methods Mod. Phys. **22**(11), 2550073 (2025). DOI: 10.1142/S0219887825500732.

[44] B. Thakran, P. K. Dhankar, S. Raut, S. Ray, S. K. Maurya and A. Sanyal, “Cosmological constraints on interacting holographic dark energy and extended Chaplygin gas in higher dimensions using MCMC analysis,” Int. J. Geom. Methods Mod. Phys. 2550254 (2025). DOI: 10.1142/S0219887825502548.

[45] P. K. Dhankar, A. Munyeshyaka, A. Sanyal, S. Islam and F. Rahaman, “Constraints on multi-fluid cosmology in modified Gauss-Bonnet gravity models with different observational data sets,” arXiv preprint arXiv:2507.22191 (2025). DOI: 10.48550/arXiv.2507.22191.

[46] P. K. Dhankar, A. Sanyal, A. Munyeshyaka, S. Ray and B. Pourhassan, “Observational analysis of bulk viscous modified Chaplygin gas in (2+1)-dimensional universe using MCMC,” arXiv preprint arXiv:2504.18612 (2025). DOI: 10.48550/arXiv.2504.18612.

[47] M. Thakre, P. K. Dhankar, B. Pourhassan and S. Islam, “Viscous Fluid Models of Cosmic Acceleration in FRW Spacetime Using MCMC Constraints,” arXiv preprint arXiv:2511.03258 (2025). DOI: 10.48550/arXiv.2511.03258.

[48] P. K. Dhankar, A. Sanyal, S. Islam, F. Rahaman and B. Pourhassan, “Testing the Generalized Second Law in $(2+1)$-Dimensional Cosmology: Holographic Entropy Bounds and Observational Constraints,” arXiv preprint arXiv:2508.13227 (2025). DOI: 10.48550/arXiv.2508.13227.

[49] D. Kumar, P. K. Dhankar, S. Ray and F. Zhang, “Joint analysis of constraints on f (R) parametrization from recent cosmological observations,” Phys. Dark Universe **49**, 101989 (2025). DOI: 10.1016/j.dark.2025.101989.

[50] M. Mune, P. K. Dhankar, S. Islam, B. Pourhassan, M. Aamir and F. Haroon, “Statistical Constraints on Anisotropic Bianchi-III Cosmology in $f(R,T)$-Gravity Using MCMC Methods,” arXiv preprint arXiv:2510.19852 (2025). DOI: 10.48550/arXiv.2510.19852.

[51] R. Patel, P. K. Dhankar, S. Islam and M. Aamir, “Data analysis in $(2+1)$-D $\Lambda(z)$ gravity with BAO, Pantheon and Hubble dataset using MCMC method,” Indian J. Phys. 1 (2026). DOI: 10.1007/s12648-026-03982-0.

[52] M. Thakre, P. K. Dhankar, S. Islam and S. Mukhtar, “Bayesian analysis of viscous modified cosmic Chaplygin gas in FRW universe with a cosmological constant,” Sci. Rep. (2026). DOI: 10.1038/s41598-026-63741-3.

[53] M. Thakre, P. K. Dhankar, A. Munyeshyaka and S. Islam, “Cosmological dynamics of f (R, G) gravity with dark sector coupling and observational analysis,” Astrophys. Space Sci. **371**(7), 83 (2026). DOI: 10.1007/s10509-026-04613-0.

[54] A. Munyeshyaka, P. K. Dhankar, V. K. Bhardwaj, S. Ray and J. Ntahompagaze, “Redshift-space distortion in modified Gauss–Bonnet gravity,” Eur. Phys. J. C **86**(8), 933 (2026). DOI: 10.1140/epjc/s10052-026-16157-2.

Article in press

[55] G. N. Gadbail, S. Arora, P. Kumar and P. K. Sahoo, “Interaction of divergence-free deceleration parameter in Weyl-type f (Q, T) gravity,” Chin. J. Phys. **79**, 246 (2022). DOI: 10.1016/j.cjph.2022.09.005.

[56] C. Chawla, R. K. Mishra and A. Pradhan, “Anisotropic Bianchi-I cosmological models in string cosmology with variable deceleration parameter,” arXiv preprint arXiv:1203.4014 (2012). DOI: 10.48550/arXiv.1203.4014.

[57] A. Pradhan, “Two-fluid atmosphere from decelerating to accelerating Friedmann–Robertson–Walker dark energy models,” Indian J. Phys. **88**(2), 215 (2014). DOI: 10.1007/s12648-013-0399-9.

[58] R. K. Mishra, A. Chand and A. Pradhan, “Dark energy models in f (R, T) theory with variable deceleration parameter,” Int. J. Theor. Phys. **55**(2), 1241 (2016). DOI: 10.1007/s10773-015-2766-0.

[59] R. K. Mishra and A. Chand, “Cosmological models in alternative theory of gravity with bilinear deceleration parameter,” Astrophys. Space Sci. **361**(8), 259 (2016). DOI: 10.1007/s10509-016-2837-6.

[60] A. G. Riess, A. V. Filippenko, P. Challis, A. Clocchiatti, A. Diercks, P. M. Garnavich, *et al.*, “Observational evidence from supernovae for an accelerating universe and a cosmological constant,” Astron. J. **116**(3), 1009 (1998). DOI: 10.1086/300499.

[61] M. Chevallier and D. Polarski, “Accelerating universes with scaling dark matter,” Int. J. Mod. Phys. D **10**(02), 213 (2001). DOI: 10.1142/S0218271801000822.

[62] M. Koussour, N. Myrzakulov, S. H. Shekh and M. Bennai, “Quintessence Universe and cosmic acceleration in f (Q, T) gravity,” Int. J. Mod. Phys. D **31**(16), 2250115 (2022). DOI: 10.1142/S0218271822501152.

[63] R. R. Caldwell and E. V. Linder, “Limits of quintessence,” Phys. Rev. Lett. **95**(14), 141301 (2005). DOI: 10.1103/PhysRevLett.95.141301.

[64] S. Tsujikawa, “Quintessence: a review,” Class. Quantum Gravity **30**(21), 214003 (2013). DOI: 10.1088/0264-9381/30/21/214003.

[65] V. Sahni, A. Shafieloo and A. A. Starobinsky, “Two new diagnostics of dark energy,” Phys. Rev. D **78**(10), 103502 (2008). DOI: 10.1103/PhysRevD.78.103502.

[66] C. Blake, S. Brough, M. Colless, C. Contreras, W. Couch, S. Croom, *et al.*, “The WiggleZ Dark Energy Survey: Joint measurements of the expansion and growth history at z< 1,” Mon. Not. R. Astron. Soc. **425**(1), 405 (2012). DOI: 10.1111/j.1365-2966.2012.21473.x.

[67] S. Arora and P. K. Sahoo, “Revisiting kink-like parametrization and constraints using OHD/Pantheon+/BAO samples,” Phys. Dark Universe **45**, 101510 (2024). DOI: 10.1016/j.dark.2024.101510.

[68] S. Mandal, P. K. Sahoo and J. R. Santos, “Energy conditions in f (Q) gravity,” Phys. Rev. D **102**(2), 024057 (2020). DOI: 10.1103/PhysRevD.102.024057.

[69] S. Capozziello, S. Nojiri and S. D. Odintsov, “The role of energy conditions in f (R) cosmology,” Phys. Lett. B **781**, 99 (2018). DOI: 10.1016/j.physletb.2018.03.064.

Article in press

[70] A. Zhadyranova, M. Koussour, Z. Kanibekova, V. Zhumabekova, U. Ismail, S. Muminov and J. Rayimbaev, "Divergence-free deceleration and energy conditions in non-minimal f (R, T) gravity," Int. J. Geom. Methods Mod. Phys. **23**(02), 2550154 (2026). DOI: 10.1142/S0219887825501543.

[71] M. Mune, P. K. Dhankar, G. Manna, S. Islam, B. Samanta and B. Pourhassan, "Observational Constraints on $f(Q,T)$ Gravity in the Presence of DBI-Essence Scalar Field," arXiv preprint arXiv:2606.21839 (2026). DOI: 10.48550/arXiv.2606.21839.

[72] P. K. Dhankar, M. Albert, S. Hussain, M. Tom and N. Joseph, "Large scale structure power spectrum and constraining model parameters in $f(Q,\mathcal{L}m)$ gravity by MCMC method," Int. J. Geom. Methods Mod. Phys. (2026). DOI: 10.1142/S0219887826502646.

[73] A. Munyeshyaka, P. K. Dhankar, M. Thakre, S. Islam, F. Rahaman and B. Pourhassan, "Background and Perturbation Constraints on Power-Law and Exponential f (G) Gravity Models from Recent Cosmological Observations," Phys. Dark Universe 102370 (2026). DOI: 10.1016/j.dark.2026.102370.

[74] M. Thakre, P. K. Dhankar, A. Munyeshyaka and S. Islam, "Testing Logarithmic f (G) Model with Observational Data Sets," J. Hologr. Appl. Phys. **6**(4), 185 (2026).

[75] P. K. Dhankar, S. Islam, S. Ray, A. Sanyal and S. K. Maurya, "Observational constraints on holography in $(2+1)$-dimensional cosmology with a generalized equation of state," arXiv preprint arXiv:2508.11701 (2025). DOI: 10.48550/arXiv.2508.11701.

[76] R. Patel, P. K. Dhankar, S. Islam, A. Munyeshyaka, S. Mukhtar and M. Ali, "Bayesian Analysis of Viscous FRW Cosmology with Inhomogeneous Equation of State," Mathematics **14**(11), 1888 (2026). DOI: 10.3390/math14111888.

[77] A. Munyeshyaka, P. K. Dhankar, A. Sanyal, S. Islam, F. Rahaman and B. Pourhassan, "Constraining f (G) gravity models using MCMC method," Phys. Dark Universe 102246 (2026). DOI: 10.1016/j.dark.2026.102246.

[78] C. Zhang, H. Zhang, S. Yuan, S. Liu, T. J. Zhang and Y. C. Sun, "Four new observational H (z) data from luminous red galaxies in the Sloan Digital Sky Survey data release seven," Res. Astron. Astrophys. **14**(10), 1221 (2014). DOI: 10.1088/1674-4527/14/10/002.

[79] J. Simon, L. Verde and R. Jimenez, "Constraints on the redshift dependence of the dark energy potential," Phys. Rev. D **71**(12), 123001 (2005). DOI: 10.1103/PhysRevD.71.123001.

[80] M. Moresco, A. Cimatti, R. Jimenez, L. Pozzetti, G. Zamorani, M. Bolzonella, *et al.*, "Improved constraints on the expansion rate of the Universe up to z$\sim$ 1.1 from the spectroscopic evolution of cosmic chronometers," J. Cosmol. Astropart. Phys. **2012**(08), 006 (2012). DOI: 10.1088/1475-7516/2012/08/006.

[81] M. Moresco, L. Pozzetti, A. Cimatti, R. Jimenez, C. Maraston, L. Verde, *et al.*, "A 6 % measurement of the Hubble parameter at z$\sim$ 0.45: direct evidence of the epoch of cosmic re-acceleration," J. Cosmol. Astropart. Phys. **2016**(05), 014 (2016). DOI: 10.1088/1475-7516/2016/05/014.

Article in press

[82] D. Stern, R. Jimenez, L. Verde, M. Kamionkowski and S. A. Stanford, "Cosmic chronometers: constraining the equation of state of dark energy. I: H (z) measurements," J. Cosmol. Astropart. Phys. **2010**(02), 008 (2010). DOI: 10.1088/1475-7516/2010/02/008.

[83] M. Moresco, "Raising the bar: new constraints on the Hubble parameter with cosmic chronometers at z$\sim$ 2," Mon. Not. R. Astron. Soc. Lett. **450**(1), L16 (2015). DOI: 10.1093/mnrasl/slv037.

[84] L. Chen, Q. G. Huang and K. Wang, "Distance priors from Planck final release," J. Cosmol. Astropart. Phys. **2019**(02), 028 (2019). DOI: 10.1088/1475-7516/2019/02/028.

[85] N. Aghanim, Y. Akrami, M. Ashdown, J. Aumont, C. Baccigalupi, M. Ballardini, *et al.*, "Planck 2018 results-VI. Cosmological parameters," Astron. Astrophys. **641**, A6 (2020). DOI: 10.1051/0004-6361/201833910.

[86] S. Alam, M. Aubert, S. Avila, C. Balland, J. E. Bautista, M. A. Bershady, *et al.*, "Completed SDSS-IV extended Baryon Oscillation Spectroscopic Survey: Cosmological implications from two decades of spectroscopic surveys at the Apache Point Observatory," Phys. Rev. D **103**(8), 083533 (2021). DOI: 10.1103/PhysRevD.103.083533.

[87] M. Abdul Karim, J. Aguilar, S. Ahlen, S. Alam, L. Allen, C. A. Prieto, *et al.*, "DESI DR2 results. II. Measurements of baryon acoustic oscillations and cosmological constraints," Phys. Rev. D **112**(8), 083515 (2025). DOI: 10.1103/tr6y-kpc6.

[88] D. Sapone and S. Nesseris, "Outliers in DESI BAO: Robustness and cosmological implications," Phys. Rev. D **112**(6), 063523 (2025). DOI: 10.1103/yknm-xskb.

[89] S. Perlmutter, G. Aldering, G. Goldhaber, R. A. Knop, P. Nugent, P. G. Castro, *et al.*, "Measurements of Ω and Λ from 42 high-redshift supernovae," Astrophys. J. **517**(2), 565 (1999). DOI: 10.1086/307221.

[90] D. Rubin, G. Aldering, M. Betoule, A. Fruchter, X. Huang, A. G. Kim, *et al.*, "Union through UNITY: cosmology with 2000 SNe using a unified Bayesian framework," Astrophys. J. **986**(2), 231 (2025). DOI: 10.3847/1538-4357/adc0a5.

[91] T. J. Hoyt, D. Rubin, G. Aldering, S. Perlmutter, A. Cuceu and R. Gupta, "Union3. 1: Self-consistent Measurements of Host Galaxy Properties for 2000 Type Ia Supernovae," arXiv preprint arXiv:2601.19424 (2026). DOI: 10.48550/arXiv.2601.19424.

[92] V. C. Busti, C. Clarkson and M. Seikel, "Evidence for a lower value for H 0 from cosmic chronometers data?," Mon. Not. R. Astron. Soc. Lett. **441**(1), L11 (2014). DOI: 10.1093/mnrasl/slu035.

Article in Press